



Using finite element modeling to design and to evaluate antiknock performance of a safety pod working in low depth tunnels

Original
Article

Mohamed H. Mabrouk, Sherif M. Abdelkhalek, Mootaz Abo-Elnor

Military Technical College

Keywords:

Evaluation of anti-knock performance, heavy mechanical equipment component, mining safety equipment, personal safety systems (PSS), survival capsule.

Corresponding Author:

Mohamed H. Mabrouk, Military
Technical College, Tel: +201011345207,
Email: mmabrouk@mtc.edu.eg

Abstract

Safety pods have recently played a vital role in protecting personnel who work in the operations that are related to tunneling and ditching in a way that they become indispensable for many mining facilities. This paper presents the design and implementation of a safety pod that can be used in low depth tunnels. The strategy of using finite element modeling to help in developing the preliminary design of the pod chassis structure has been discussed. A computer model of the safety pod chassis structure has been developed to refine the design and the simulation results show satisfactory safety factors under the expected loads. The full-scale pod has been built by a specialized contractor according to heavy protection equipment standards with considering the safety precautions and providing all documents related to inspection and maintenance to assure pod long service life as well as safe operation. The full details of the pod implementation process, used materials, material testing results, and the manufacturing stages according to detail drawings and blueprints are considered out of scope of this article and is going to be published in our upcoming article.

I. INTRODUCTION

The usage of safety equipment such as survival capsule, safety pods and refuge chambers have become vital in the field of mining and tunnels' construction to protect personnel in case of tunnel collapses or soil failures in a way that decreases accidents, miners' injuries, and death rates^[1].

In spite of their capability to meet the safety standards of the mining operations, some of safety equipment such as refuge capsules are rather expensive as they are designed to be used to protect miners when working in missions of challenging nature such as working in hazardous environment in a way that affects the economical feasibility of using those equipment in field. A safety pod, however, is economical safety equipment that is recommended to be used especially for normal working environmental parameters. Those pods have been extensively used during the construction of non-deep trenches^[2-4].

Safety pods have proved efficient to protect and rescue miners during many underground collapse accidents. A standard safety pod is designed to shelter up to four people offering them survival protection against underground collapse incidents and sudden soil failures through its durable rigid structure, reliable design, optimized weight, and compact size. These features can be achieved by using high strength with low weight materials to manufacture

such equipment to allow carrying the pod with a standard mobile crane in case of low and moderate digging operations with low risk margins. The design of safety pods should be verified and tested to make sure that they achieve the standard safety precautions that guarantee efficient operation when needed^[5].

It is important to evaluate the safety pod antiknock performance through modeling and simulation analysis considering that the risk margin would be high if the pod is poorly designed. Also to prepare the safety pod to face the challenging factors such as exposure to high momentum loads due to soil collapses, it is crucial to perform accurate evaluation for the structural safety during the design procedures of the pod^[5].

Many studies have been proceeded to determine the antiknock sustain performance for safety equipment, soil failure mechanisms parameters, and the characteristics of stresses and deformations. Studies with theoretical background mostly use numerical simulations^[6-8] while researches with experimental basis mainly depend on measuring the stresses and displacement values for a full scale safety equipment prototype^[8-9]. Numerical simulations provide an economic method to evaluate the antiknock performance of safety pods as the full-scale experimental evaluation is relatively of high cost.



Fig. 1: Safety pod (courtesy of Solent® News and photo agency)

The motive of the research presented in this paper is the incident that took place in Egypt, when a low depth trench collapsed over one of the researchers causing his death. The trench wasn't so deep but the lack of using a safety pod designed to work in low depth tunnels led to that tragic result.

The key point in this paper is to develop a finite element

model to aid for refinement of the pod proposed design in the final design phase. Also, to use the model to evaluate the pod anti-knock performance under the expected loads exerted on it due to the sudden collapse of a tunnel and hence to assure its reliability to protect the personnel inside in such incidents. To design the safety pod, the approach followed in^[5] is used here.

The paper is arranged as follows; section II is devoted to present the proposed design of the safety pod structure followed by the developing of a finite element model to verify the pod structure design as discussed in section III. Section IV is devoted to present the simulation results to ensure the reliability of the pod proposed design in case of abrupt tunnel failure. The manufacturing of the full-scale pod is presented in section V.

II. PROPOSED DESIGN OF THE SAFETY POD

The main causes of soil failures are generally the poor geological parameters, the unstable discrimination of geological environment and the groundwater erosion. Over the years, strict safety standards for safety equipment have been made by researchers and have been adopted in manufacturing countries^[3-4] to make sure that the pod structural durability can sustain the disastrous environment challenging factors such as soil failure and high temperature.

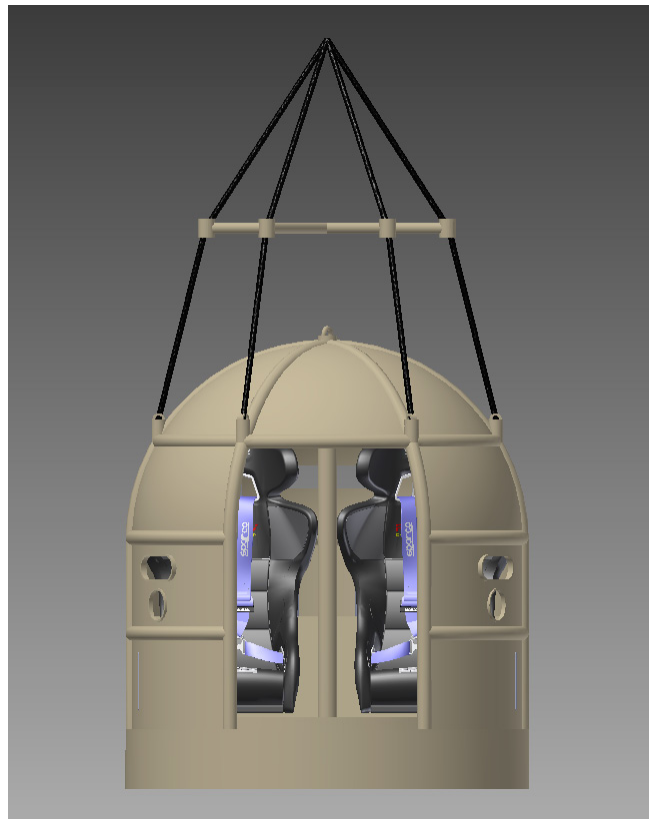


Fig. 2: Proposed design of the safety pod



The proposed design here is compatible with safety equipment design standards^[10]. The proposed design of the safety pod is executed with the aid of Autodesk Inventor®, as shown in Figure 2. Using finite element numerical analysis, the stability characteristics of safety pod structure in case of tunnel collapse are discussed in section IV using the simulation results presented later in this paper.

In the case of tunnel collapse, there are many factors that determine the stresses a safety pod may be exposed to. However, the stresses exerted upon the safety pod structure are only in one direction in the case considered in this paper; when low depth tunnel collapses^[11].

III. FINITE ELEMENT MODEL

Finite element method (FEM), which is considered numerical solution of complex problems in structural mechanics, has been extensively used for mathematical modeling of engineering systems in many fields such as terra-mechanics, aeronautical and automotive industries. Considering an applied system structure, the method helps in checking deformations, stiffness and strength for a proposed design as well as in minimizing materials weight.

The virtual work principle approach is the one of the most widely used perspectives of the FEM for structural analysis due to its applicability to both linear and non-linear material behaviors. The virtual work method can be expressed for a stable system as the summation of external forces work exerted upon the system equal to the work stored as strain energy in the system constituents^[12-13].

Subsequently, the principle of virtual displacement for safety pod structure can be used to mathematically represent the external virtual work as

$$\text{External virtual work} = \int_V \delta \epsilon^T \sigma dV \quad (1)$$

The internal virtual work can be determined by calculating the summation of the virtual work done on the individual elements that constitute the pod structure. Therefore, the displacement of the structure can be represented by the collective response of the elements.

The equations are written here for the domain of individual elements of the safety pod structure instead of using a single equation that represent the continuum response of the system. Hence, the equilibrium equation can be expressed as

$$\mathbf{R} = \mathbf{K}\mathbf{r} + \mathbf{R}^o \quad (2)$$

The nodal displacements are calculated by solving equation (2), subsequently

$$\mathbf{r} = \mathbf{K}^{-1} (\mathbf{R} - \mathbf{R}^o) \quad (3)$$

The strains and stresses for each individual element are calculated as:

$$\epsilon = \mathbf{B}\mathbf{a} \quad (4)$$

$$\sigma = \mathbf{E}(\epsilon - \epsilon^o) + \sigma^o = \mathbf{E}(\mathbf{B}\mathbf{a} - \epsilon^o) + \sigma^o \quad (5)$$

Where \mathbf{R} is the nodal forces vector, \mathbf{K} is the stiffness matrix of safety pod structure, \mathbf{r} is the safety pod structure nodal displacement vector, \mathbf{R}^o is the equivalent nodal forces vector, \mathbf{B} is the strain-displacement matrix, \mathbf{E} is the safety pod elasticity matrix, ϵ^o is the vector of initial strains in the element, σ^o is the vector of initial stress in the element.

Matrices such as \mathbf{B} , \mathbf{K}^e , \mathbf{R}^o and \mathbf{K} are related to system elements and can be determined by applying equation (1) to the safety pod structure system while matrices such as ϵ^o , σ^o , \mathbf{R} , \mathbf{E} can be directly set up from data input as they are standard data for the safety pod structure material. The displacement at any other point of each element is calculated using the following interpolation function:

$$\mathbf{u} = \mathbf{N}\mathbf{q} \quad (6)$$

Where \mathbf{u} is the displacements vector for an element at any point (x,y,z) , \mathbf{N} (the matrix of shape functions) is serving as interpolation functions. Since the nodal displacement vector \mathbf{q} is a subset of the system nodal displacement \mathbf{r} , the internal virtual work due to virtual displacements for an element of volume V^e is calculated as:

$$\text{Internal virtual work} = \delta \mathbf{r}^T (\mathbf{K}^e \mathbf{r} + \mathbf{Q}^{oe}) \quad (7)$$

Where:

$$\mathbf{K}^e = \int_{V^e} \mathbf{B}^T \mathbf{E} \mathbf{B} dV^e \quad (8)$$

$$\mathbf{Q}^{oe} = \int_{V^e} -\mathbf{B}^T (\mathbf{E} \epsilon^o - \sigma^o) dV^e \quad (9)$$

Therefore, the internal virtual work of the safety pod structure

$$= \delta \mathbf{r}^T (\sum_e \mathbf{k}^e) \mathbf{r} + \delta \mathbf{r}^T \sum_e \mathbf{Q}^{oe} \quad (10)$$

Where \mathbf{K} is the pod structure stiffness matrix ($= \sum_e \mathbf{k}^e$)

While \mathbf{R}^o is the vector of equivalent nodal forces

$$(\mathbf{R}^o = \sum_e \mathbf{Q}^{oe} + \mathbf{Q}^{te} + \mathbf{Q}^{fs})$$

IV. SIMULATION RESULTS

Safety pods are designed to face challenging circumstances to protect people inside against emergency

situations that may cause their death. While full-scale experimental antiknock performance evaluation for safety pods is considered as time-consuming relatively expensive approach, numerical simulation provides a feasible way for conducting such analysis. Hence, it is important to achieve close to real antiknock performance analysis for the pod through modeling and simulation.

Numerical simulation approach has been used extensively to predict the behaviour of the safety pods in cases of emergency situations such as soil failure. This approach proves to be cost effective and reliable to be used to evaluate the design of the pod. Numerical simulation data analysis results, especially the pod structure displacement

and total deformation characteristics in case of soil failure, is used here to determine the antiknock performance of the safety pod to examine the pod design presented in this paper^[5]. In this research, the approach adopted in^[11] is used and the safety pod is designed to face the abrupt collapse of a low depth tunnel with the assumption that the stresses are exerted mainly on the safety pod dome radial direction. The predicted radial stresses have been calculated using the safety pod main dimensions, tunnel depth, and the soil general characteristics. The exertion of the calculated stresses upon the pod is then simulated using the developed finite element model with the aid of Autodesk Inventor®, as shown in Figure 3.

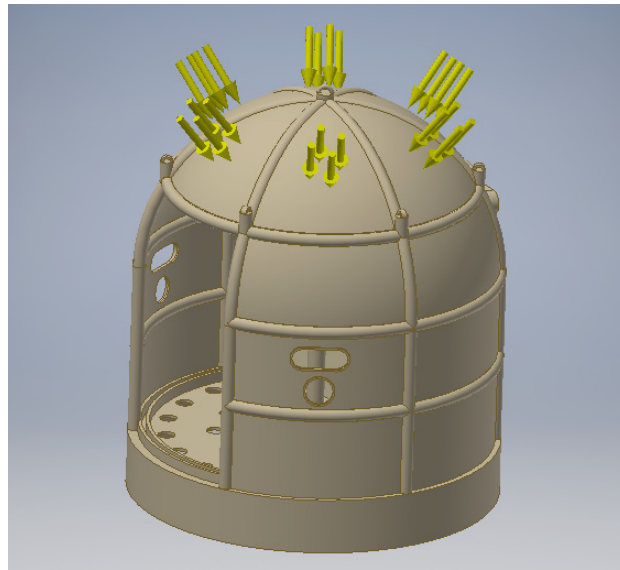


Fig. 3: The predicted stresses exerted on pod due to tunnel collapse

Figure 4 shows the simulation of the case scenario in which the pod is under the influence of static load equals to the weight of earth column over the pod dome. The numerical simulation results shown in Figure 4 represent

the pod total deformation characteristics under static load applied on the pod for soil failure situation in cases of collapsing tunnels whose depths ranges from 3 m to 15 m depth tunnel.

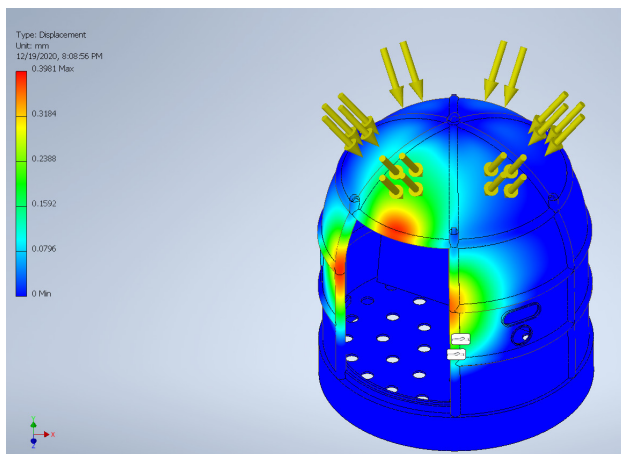


Fig. 4: (a) Pod displacement due to tunnel collapse (3 m depth)

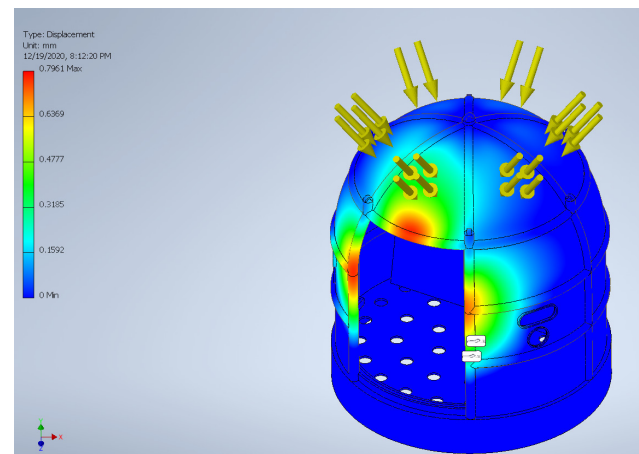


Fig. 4: (b) Pod displacement due to tunnel collapse (7 m depth)

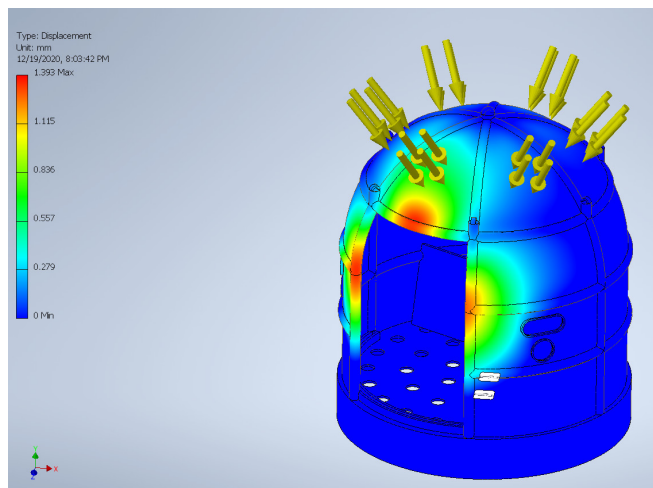


Fig. 4: (c) Pod displacement due to tunnel collapse (13 m depth)

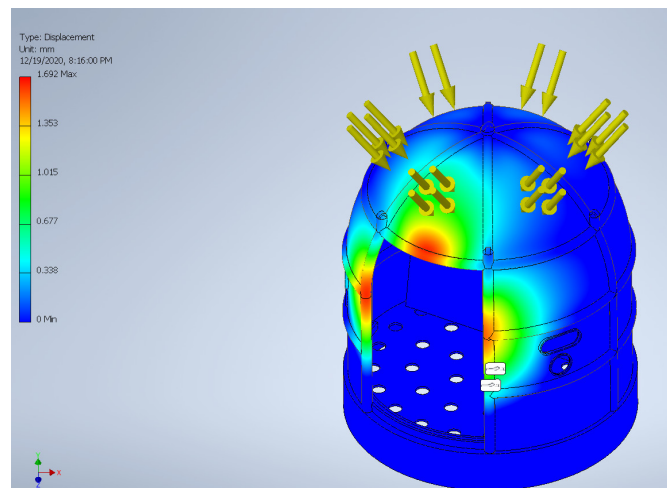


Fig 4: (d) Pod displacement due to tunnel collapse (15 m depth)

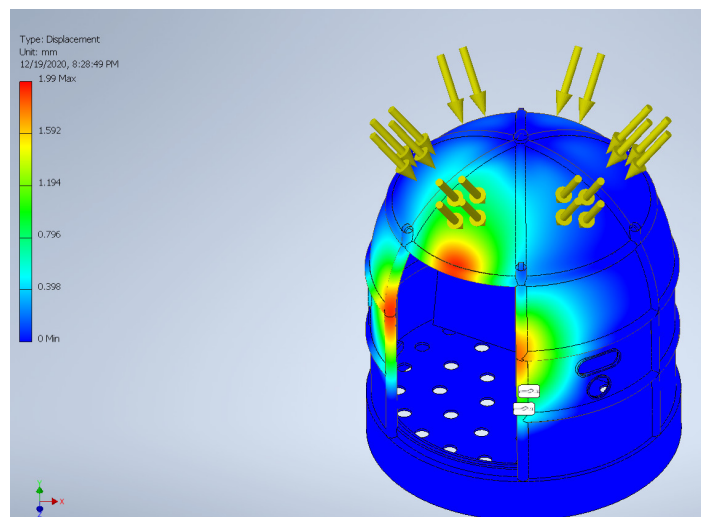


Fig. 4: (e) Pod displacement due to tunnel collapse (20 m depth)

Fig. 4: Simulation results for pod displacement under static load due to tunnel collapse

From results shown in Fig. 4, it can be seen that the maximum displacement in the pod is expected to range from (0.39) mm to (1.9) mm in case after 3m depth tunnel collapse to 20m depth tunnel collapse, respectively. This confirms the reliable design of the pod as well as its rigid structure that enables it to protect the people inside.

The numerical simulation results, represented in Fig.5 using ANSYS®, show the pod total deformation characteristics with time that ranges from 0.00344sec to 1sec measured after abrupt 15m depth tunnel collapse

while the pod is in there represented by exerting a dynamic load on the pod. Equations (1-10) are used to estimate the pod structure deformation in different parts while equations from^[14] are used to calculate the stress loads that have been used in the simulation. It is worth noting that the results conclude that the total deformation of the pod doesn't change after time equal 1 sec, the results also show that the proposed design can sustain the load to an extent that makes the pod structure total deformation doesn't exceed the value of 0.6068 mm in worst case scenarios.

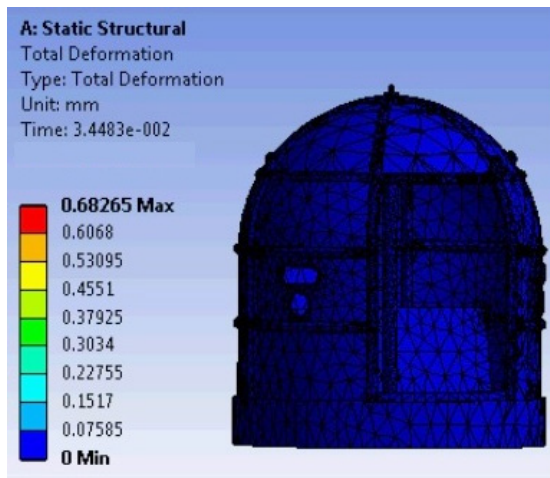


Fig. 5: (a) Pod total deformation at $t = 0.0034$ sec after tunnel failure.

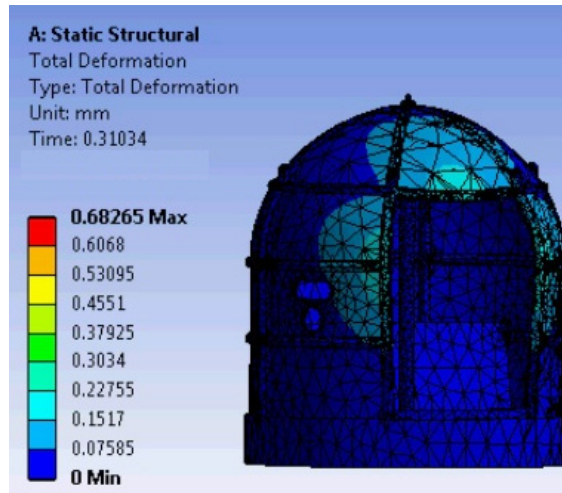


Fig. 5: (b) Pod total deformation at $t = 0.31$ sec after tunnel failure

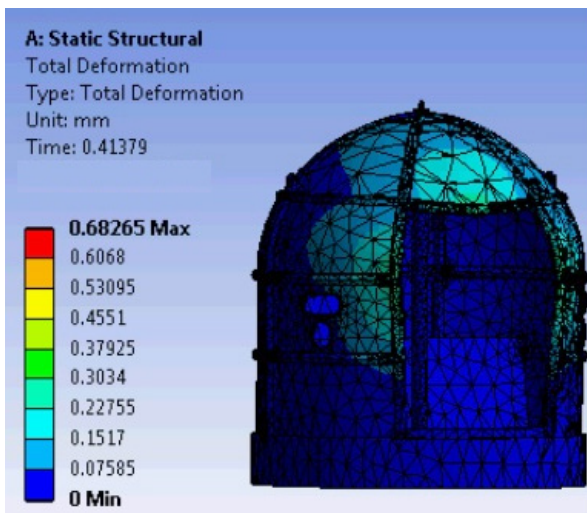


Fig. 5: (c) Pod total deformation at $t = 0.41$ sec after tunnel failure

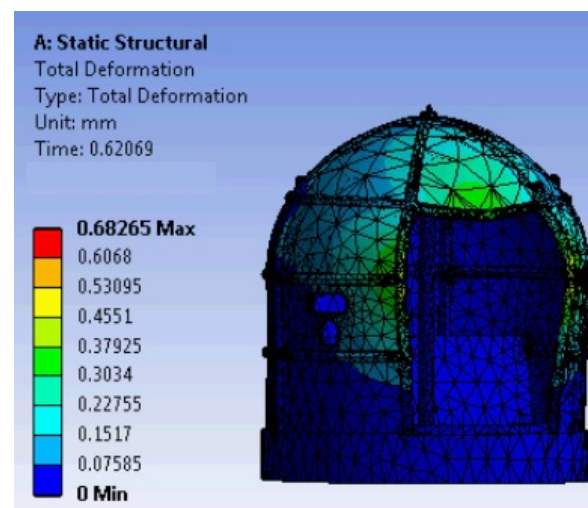


Fig. 5: (d) Pod total deformation at $t = 0.62$ sec after tunnel failure

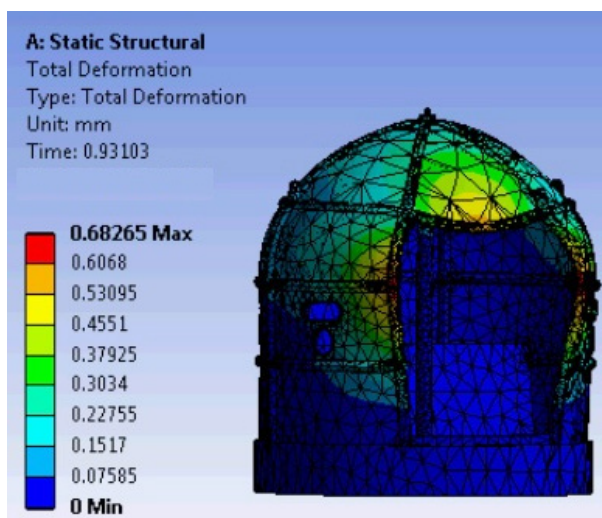


Fig. 5: (e) Pod total deformation at $t = 0.93$ sec after tunnel failure

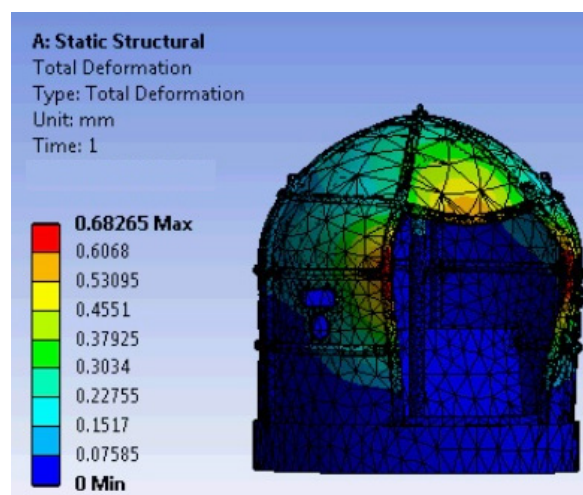


Fig. 5: (f) Pod total deformation at $t = 1$ sec after tunnel failure

Fig. 5: Simulation results pod total deformation with time after tunnel failure

To assure the reliability of the pod design, the safety factor distribution over the different parts of the pod structure is studied, Fig.6 shows the simulation results pod structure safety factors under static load due to tunnel collapse. The simulation results are calculated for expected safety factors in the case scenario in which the pod is under the influence of static load equals to the weight

of earth column over the pod dome. The numerical simulation results shown in Figure 6 represent the pod safety factors distributed all over the pod structure when influenced by static load applied on the pod after soil failure situation in cases of collapsing tunnels whose depths ranges from 3 m to 20 m depth tunnel.

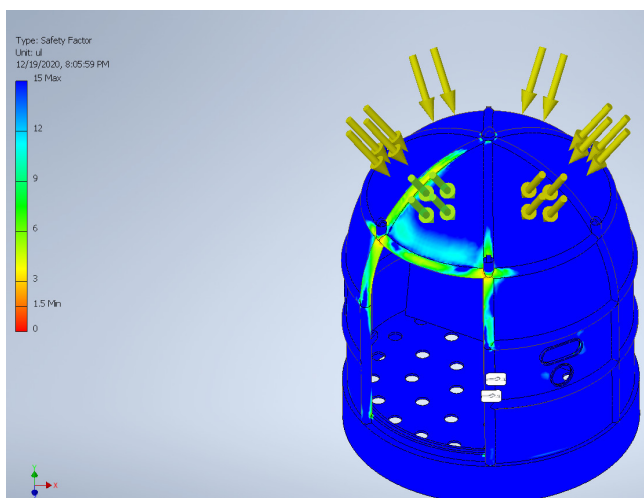


Fig. 6: (a) Simulation results (pod structure safety factors) under static load (3 m depth tunnel failure)

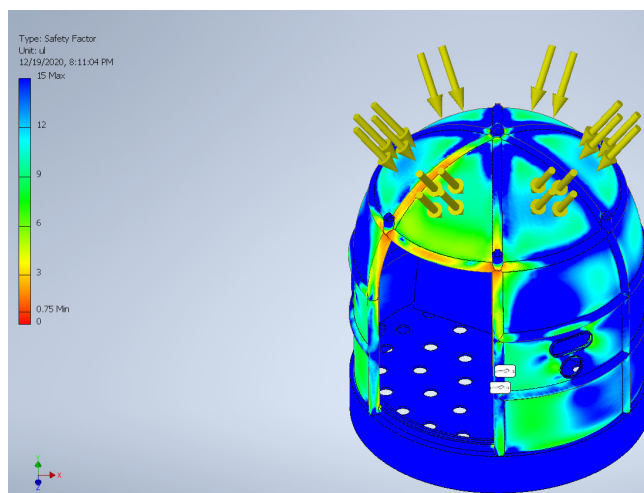


Fig. 6: (b) Simulation results (pod structure safety factors) under static load (7 m depth tunnel failure)

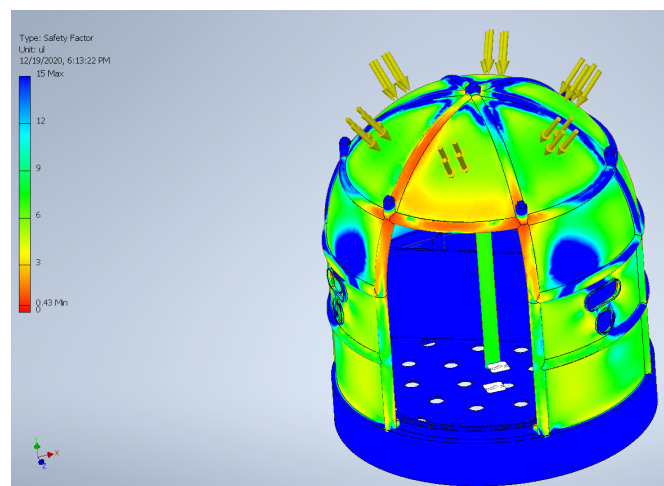


Fig. 6: (c) Simulation results (pod structure safety factors) under static load (13 m depth tunnel failure)

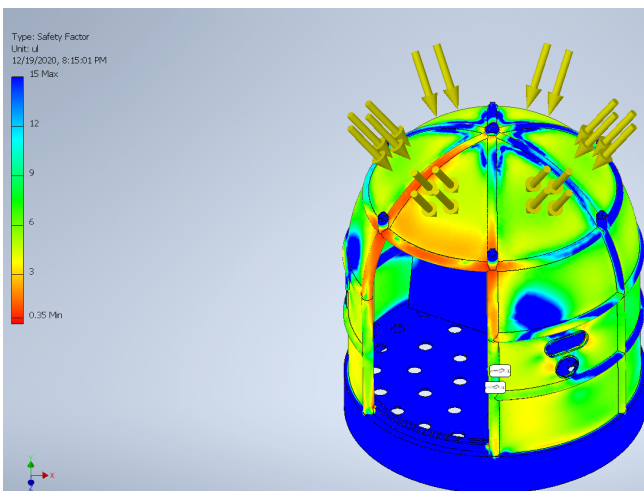


Fig. 6: (d) Simulation results (pod structure safety factors) under static load (15 m depth tunnel failure)

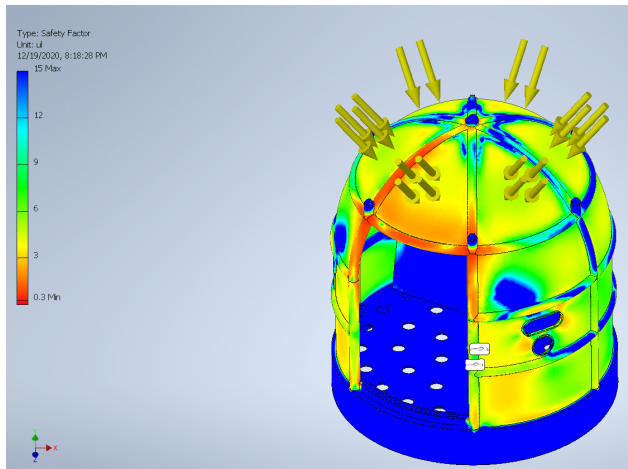


Fig. 6: (e) Simulation results (pod structure safety factors) under static load (20 m depth tunnel failure)

Fig. 6: Simulation results for pod structure safety factors under static load due to tunnel failure.

From the results shown in Figure 6, it can be inferred that the minimum safety factor in the pod is expected to range from (4) to (1.2) in case of abrupt collapse of tunnels ranging in depth from 3m depth tunnel to 20m depth tunnel, respectively. The safety factor is expected to be less than 1.5 in some regions in the vicinity of the welding points in the pod structure near the dome when the 20m tunnel collapses. Therefore, the pod is recommend to be used to protect people in a tunnel of depth lower than 15 m, Figure 7 shows the values of the minimum safety factors versus the depth of the collapsed tunnel.

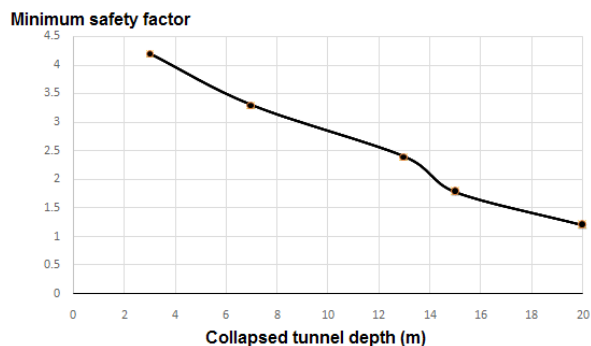


Fig. 7: Simulation results for pod structure minimum safety factors under static load versus the depth of the collapsed tunnel.

V. FULL-SCALE POD MANUFACTURING

In this research, the same approach followed in^[5] is used for the pod manufacturing. The safety pod proposed design presented in this paper and all outcome working drawings and calculation reports, design reports, blueprints have been passed to heavy duty equipment manufacturers' requirements compliant contractor. The contractor builds the pod according to implements requirements criteria from the safety regulations, optimum manufacturing of

heavy duty equipment governed by the Occupational Safety and Health Administration (OSHA) regulations, and the American Society of Mechanical Engineers (ASME) standards^[15-17].

Safety pod maintenance archive file information provide a source of monitoring pod structure condition with time to show if there is a trending pattern of deterioration, rust, wear, or other factors that may compromise the safe use of the pod. The maintenance archive file of the pod, which includes all documents related to the pod inspection, evaluation, maintenance and repair, has been developed. The file includes documents such as pod daily inspection checklist, post-operative inspection checklist, testing records, evaluation records, maintenance records, and repair records. Keeping an updated archive maintenance filing system is important to provide an evidence of a safe and reliable use of the pod.

The pod consists of three main parts, which are pod skeleton, covering sheets, and the base that hold the three chairs and the supply storage, as shown in Figures 8-9. The pod skeleton holds all the pod parts together and is considered as the supporting backbone of the pod. It contains multi-hook rings at different locations to help hoisting the pod with a standard mobile crane. The skeleton is made of circular cross section welded tubes that are supported together by number of joints, which are made of square cross section beams. The base structure is made of steel I-beam cross-sectional parts welded to form the required designed base shape.

Considering the fact that the pod is to be operated in emergency situations in which it may be exposed to impact loads also the fact that the pod is a dangerous piece of equipment, it is crucial to follow basic heavy equipment hazard prevention measures that ensure the safety of all personnel inside. The pod load test report and load chart have been developed as a result of proceeding the load test for the pod with calibrated load measuring devices and all design sheets, calculations and dimensions have been double checked and proofed to be accurate within acceptable tolerance.

The high strength low weight manufactured safety pod can host up to (3) persons, as shown in Figure 8-9. The standard features of the pod according to the proposed design include pod internal light, multiple hook hoisting points on the pod outer surface, shoulder harnesses and seat belts to assure safety seating, storage space (sufficient for two day's supply per person), single hatch design, air ventilation vents, air supply tank, hard restraint support, internal thermal insulation, and internal personnel chock cushion. The upcoming future upgrade features include ground and rooftop tether system, solar panel array, underground GPS (global positioning system) tracking system. The full details of the pod implementation process, used materials, material testing results, and the manufacturing stages according to detail drawings and blueprints are considered out of scope of this article and is going to be published in our upcoming article.



Fig. 8: (a) Manufactured safety pod main door and hatches



Fig. 8 : (b) Manufactured safety pod from inside

Fig. 8: Manufactured safety pod prototype

CONCLUSIONS

Safety pod is one of the many types of the personal safety systems that can be used especially in the mining and tunneling field to provide safety and protection to persons in case of tunnels collapse incidents until rescue crews arrive on the scene. This paper presents the use of finite element modeling and simulation to aid the design and implementation of a safety pod that can be used to protect workers in low depth tunnels and shallow mining operations. A mathematical model has been developed to evaluate the anti-knock performance of the pod chassis structure and has been used to test the pod ability to protect personnel inside in case of tunnel failure for different depths. The anti-knock performance simulations include the determination of pod structure minimum safety factors under loads expected from collapsing tunnels of different

depths as well as pod total deformation under such loads. The simulation results show that the safety pod will operate efficiently in harsh circumstances as well as its reliability to withstand the initial impact and to protect the personnel inside in case of collapse of tunnels up to 14m in depth. The pod design, which includes the construction of the pod as well as the chassis structure stress analysis, has been discussed. All calculation reports, working drawings, design reports, and blueprints resulted from work presented in this paper have been passed to a contractor to build full-scale pod according to standards that govern building of heavy protection equipment to assure pod safe operation and long service life.

VI. REFERENCES

- [1] Zhai Xiaowei, Wu Shibo, Wang Kai, Chen Xiaokun, Li Haitao, "A Novel Design of Rescue Capsule considering the Pressure Characteristics and Thermal Dynamic Response with Thermomechanical Coupling Action Subjected to Gas Explosion Load", Volume 2017, Article ID 5261309, <https://doi.org/10.1155/2017/5261309>.
- [2] Boyi Zhang, Dongxian Zhai, and Wei Wang, "Failure Mode Analysis and Dynamic Response of a Coal Mine Refuge Chamber with a Gas Explosion", *Appl. Sci.* 2016, 6, 145; doi:10.3390/app6050145.
- [3] Department of Labor, "Mine safety and health administration," *Federal Register*, vol. 73, no. 25, pp. 656–700, 2008.
- [4] Xiaoli Hao, Chenxin Guo, Yaolin Lin, Haiqiao Wang, and Heqing Liu, "Analysis of Heat Stress and the Indoor Climate Control Requirements for Movable Refuge Chambers", *Int. J. Environ. Res. Public Health* 2016, 13, 518; doi:10.3390/ijerph13050518.
- [5] Mohamed H. Mabrouk and Sherif A. AbdelKhaliq, "Design and Implementation of a Light Duty Gantry Crane", *International Journal of Engineering Research & Technology (IJERT)*, Vol. 3, Issue 12, pp.381-388. ISSN: 2278-0181
- [6] L. D. Ma, H. Y. Pan, and Y. Wang, "Numerical simulation of a refuge chamber resisting gas explosion impact," *Journal of Vibration and Shock*, vol. 31, no. 20, pp. 172–176, 2012.
- [7] Changsheng Li, Biao Ma, Tao Li, Tao Zhu, "Microstructure and Mechanical Properties of 1,000 MPa Ultra-High Strength Hot-Rolled Plate Steel for Coal Mine Refuge Chamber", *Acta Metall. Sin. (Engl. Lett.)*, 2014, 27(3), 422–429, DOI 10.1007/s40195-014-0074-y.
- [8] P. H. Guo, G. T. Jiao, and J. Han, "Anti-explosion performance and numerical simulation optimization of refuge chamber," *Mechanical Engineering & Automation*, vol. 189, no. 2, pp. 96- 97, 2015.
- [9] Hao Shao, Peng-fei Li, Xu-mao Shi, "Experimental study of the gas leakage and optimized supply of oxygen in coal mine refuge chamber", *Procedia Engineering* 211 (2018) 599-605.
- [10] Huiying WANG, Yuanyuan JIA, Lun CAO, "Cause Analysis and Prevention of Road Tunnel Collapse in Complex Soft Strata", *Energy Procedia* 16 (2012) 259-264.
- [11] M. G. Song and S. R. Ge, "Dynamic response of composite shell under axial explosion impact load in tunnel," *Thin-Walled Structures*, vol. 67, pp. 49–62, 2013.
- [12] *Theory of Matrix Structural Analysis*, J. S. Przemieniecki, McGraw-Hill Book Company, New York, 1968
- [13] Clough, R.W, "The Finite Element in Plane Stress Analysis." *Proceedings, 2nd ASCE Conference on Electronic Computations*, Pittsburgh, Sep 1960
- [14] Mohamed M. Abdeldayem, Mohamed H. Mabrouk and Motaz AboElnor, "Analytical and Numerical Modeling of Soil Cutting and Transportation During Auger Drilling Operation", *Journal of Verification, Validation and Uncertainty Quantification, Transactions of the ASME* , 2020, Vol. 5 / 021002-1.
- [15] MOU between MSHA and OSHA, "Interagency Agreement between The Mine Safety and Health Administration U.S. Department of Labor and The Occupational Safety and Health Administration U.S. Department of Labor", 1979.
- [16] ASME B20 Safety Standards for Conveyors and Related Equipment and BTH Standards Committee, *Design of Below-the-Hook Lifting Devices*
- [17] ASCE/SEI 7-16, Minimum design loads and associated criteria for building and other structures.